

## Experiments on centrifugally driven thermal convection in a rotating cylinder

By J. L. HUDSON,

Department of Chemical Engineering, University of Virginia

DANIEL TANG† AND STEVEN ABELL‡

Department of Chemical Engineering, University of  
Illinois at Urbana-Champaign

(Received 7 April 1977 and in revised form 11 October 1977)

Heat-transfer measurements have been carried out in a right circular cylinder of fluid which is heated from above and rotated steadily about its vertical axis. Convection is produced relative to solid-body rotation through the coupling of the centrifugal acceleration and density variations in the fluid. Two silicone oils having kinematic viscosities of 350 cS and 0.65 cS were used in the experiments. In the former case viscous forces are important throughout the cylinder whereas in the latter case Ekman layers form and the Coriolis acceleration controls the interior flow.

With the 350 cS oil the Nusselt number for heat transfer from the top to the bottom of the cylinder is a function of  $Gr_\omega$  and  $r_0$ , where  $Gr_\omega$  is a Grashof number defined by employing the centrifugal acceleration evaluated at the outer edge of the cylinder in place of the gravitational acceleration, and  $r_0$  is the cylinder aspect ratio.

The behaviour is quite different for the 0.65 cS oil. Ekman layers form on the horizontal surfaces and heat is convected by Ekman suction. The Nusselt number is given by

$$Nu = 4.16\beta^{0.822} \epsilon^{-0.499} r_0^{0.173}, \quad Ac \leq 0.025, \quad \sigma\beta\epsilon^{-\frac{1}{2}} > 0.7,$$

where  $\beta$  is the thermal Rossby number,  $\epsilon$  is the Ekman number,  $\sigma$  is the Prandtl number, and  $Ac$  is the ratio of gravitational to centrifugal accelerations. This is consistent with previous theories which indicate that the system should depend on the parameters  $\sigma\beta\epsilon^{-\frac{1}{2}}$  and  $r_0$  in the limit as  $\epsilon$  and  $\beta$  approach zero.

---

### 1. Introduction

The coupling of a density gradient and an acceleration acting normal to it will produce convection in a fluid. One example of this is free convection in which a horizontal temperature gradient and the vertical acceleration of gravity cause fluid motion. Similarly, the centrifugal acceleration can produce motion relative to solid-body rotation in a rotating fluid.

We have studied centrifugally driven thermal convection in a right circular cylinder of radius  $a$  and height  $d$ . The cylinder is completely filled with fluid and rotates about

† Present address: Staley Company, Decatur, Illinois.

‡ Present address: Monsanto Company, St Louis, Missouri.

its axis at a steady rate  $\omega$ . If the fluid were isothermal it would be in solid-body rotation. However, the top surface is held at a temperature  $T_a$  and the bottom at  $T_b$  where  $T_a > T_b$ . The temperature difference  $\Delta T = T_a - T_b$  is always positive so that gravitational instabilities do not occur. Because of the imposed temperature difference, heat is transferred from the top surface to the bottom surface, and the rate of heat transfer is augmented by the convection which occurs relative to solid-body rotation. The side wall of the cylinder is insulated so that any heat entering the cylinder at the top is removed at the bottom.

Thermal convection in a rapidly rotating cylinder has been treated theoretically by Barcilon & Pedlosky (1967), who present a perturbation solution for a small ratio of centrifugal to gravitational acceleration, and by Homsy & Hudson (1969, 1971*a, b*) who consider the centrifugal acceleration to be of the same order as or greater than the gravitational acceleration. The solutions are carried out by making the Boussinesq approximation and are valid for small Ekman number such that boundary layers are present on all inside surfaces of the cylinder. More recently Sakurai & Matsuda (1974), Matsuda, Hashimoto & Takeda (1976), and Nakayama & Usui (1974) have analysed compressible fluids and have discussed applications of the results to a gas centrifuge used in the enrichment of uranium.

It might be noted that motion relative to solid-body rotation is always produced by a density gradient parallel to the axis of rotation even though this flow may be smaller than those produced by other means. For example, Linden (1977) has recently reported experiments on a stratified rotating fluid where flow is produced by the differential rotation of a lid. At the low rotational rates employed ( $\omega < 1.6$  rad/s) the centrifugally driven thermal convection was small compared with the flow induced by the lid.

Because of the complicated nature of these boundary-layer flows, the results of the analyses are greatly restricted. By means of the mathematical analyses the boundary-layer nature of the flow has been determined, but quantities such as the heat flow are known only under very narrow limiting conditions. The experimental studies described in this paper were thus carried out for three reasons: (i) to determine the dependence of the heat flux (or Nusselt number) on the system parameters over a range of conditions; (ii) to verify the parametric dependence suggested by the theories and (iii) to aid in interpreting results of studies on gravitational instabilities in rotating cylinders heated from below (Rossby 1969; Tang & Hudson 1978).

For either boundary-layer or non-boundary-layer flows, the dimensionless velocity and temperature fields and thus the Nusselt number depend on five dimensionless parameters, viz. the Prandtl number  $\sigma$  and

$$\epsilon = 2\nu/\omega d^2 \quad (\text{Ekman number}),$$

$$\beta = \frac{1}{8}\alpha\Delta T \quad (\text{thermal Rossby number}),$$

$$r_0 = a/d \quad (\text{aspect ratio}),$$

$$Ac = g/\omega^2 a \quad (\text{acceleration ratio}),$$

where  $\nu$  is the kinematic viscosity,  $\alpha$  the coefficient of thermal expansion,  $g$  the gravitational acceleration, and the other quantities are as defined above (Homsy & Hudson 1969). The Nusselt number is defined by the ratio of the heat flux through the cylinder

to that flux which would occur in solid-body rotation;  $Nu$  is thus identically one for no convection and is greater than one when convection takes place.

When the Ekman number  $\epsilon$  is small, a boundary-layer flow occurs. For

$$(\epsilon, \beta, Ac) \ll 1 \quad \text{and} \quad \{r_0, \sigma\} \geq O(1),$$

the horizontal Ekman layers control the axial flow in an inviscid core, the boundary layers on the vertical wall of the cylinder have a large influence on the temperature field, and the Coriolis acceleration dominates the flow in the inviscid core (Homsy & Hudson 1969). Most important for the present study, for sufficiently small  $\beta$  the Nusselt number should depend on the parameters  $\beta$ ,  $\sigma$ , and  $\epsilon$  as the product  $\sigma\beta\epsilon^{-\frac{1}{2}}$ . In terms of dimensional quantities then, the heat flux should depend on the imposed temperature difference and the rotational rate as some function of  $\Delta T \cdot \omega^{\frac{1}{2}}$ .

When  $\epsilon$  is not small, boundary layers do not form and viscous forces are important throughout the cylinder; in this case the dependence of the Nusselt number on the parameters is quite different. Although a detailed analysis is not available, preliminary considerations indicate that the Nusselt number may depend on the same three parameters as a function of  $\sigma\beta\epsilon^{-2}$  for sufficiently small  $\beta$  (Homsy 1969). Thus the heat flux would depend on  $\Delta T$  and  $\omega$  as  $\Delta T\omega^2$ . This result indicates that the Nusselt number may be a function of a rotational Grashof number defined by replacing the acceleration of gravity by the rotational acceleration, or

$$Gr_\omega = \frac{a\omega^2\alpha\Delta Td^3}{\nu^2} = 32\frac{\beta r_0}{\epsilon^2}.$$

In this case, centrifugally driven thermal convection would behave much as its gravitational counterpart and the Coriolis acceleration would play a minor role. It should be noted that the Coriolis acceleration would also not dominate the flow for any fluid if the geometry of the container inhibits a tangential flow. This would be the case in the hollow turbine blades described by Schmidt (1951) and the tubes analysed by Lighthill (1953), or in the experiments in a rotating channel carried out by Abell & Hudson (1975).

In order to investigate the dependencies indicated above, experiments were carried out using two silicone oils having nominal kinematic viscosities of 0.65 and 350 cS respectively. With the former, the Ekman number  $\epsilon$  has values as low as  $4.26 \times 10^{-5}$  for the experiments described here. Since the thickness of the Ekman layers on the horizontal surfaces is  $O(\epsilon^{\frac{1}{2}})$ , a boundary-layer flow regime will exist. For the 350 cS oil, however, the smallest value of the Ekman number is  $2.1 \times 10^{-2}$ , so that Ekman layers are only beginning to form at the highest rotational rates.

## 2. Experiments

### 2.1. Apparatus

The test fluid is contained in a right circular cylinder which rotates about a vertical axis at a constant angular velocity  $\omega$ . The plastic vertical side wall is insulated. The top and bottom surfaces are aluminium and are heated and cooled respectively with water. Temperatures at the horizontal surfaces are measured with thermistors. Heat fluxes from the top surface to the working fluid and from the working fluid to the bottom surface are determined by measuring the temperature differences across calibrated

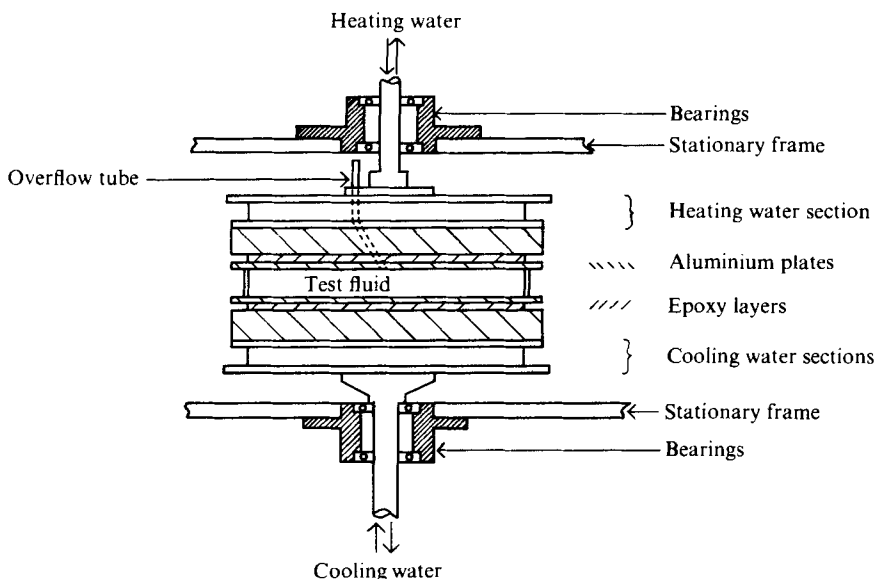


FIGURE 1. Rotating assembly.

thermal resistances. These thermal resistances consist of epoxy layers held between aluminium disks. A similar method of measuring heat fluxes was used by Rossby (1969) in studying gravitational instabilities in rotating fluids.

The cylinder is formed by two horizontal aluminium plate assemblies and a cast acrylic plastic ring (see figure 1). Two plastic rings were used such that the cylinder had a radius ( $a$ ) of 13.98 cm and a height ( $d$ ) of either 0.97 cm or 2.00 cm. Above and below the test fluid are assemblies consisting of a thin aluminium plate (in contact with the test fluid), an epoxy layer, and a thicker aluminium plate. The thicknesses of the aluminium plate, epoxy layer, and aluminium plate are 0.795 cm, 0.876 cm, and 2.45 cm for the top assembly and 0.795 cm, 0.876 cm, and 2.54 cm for the bottom assembly. A good bond between aluminium and epoxy was obtained by cleaning the aluminium with chromic acid solution and then pouring the epoxy between the aluminium disks. The aluminium surfaces were polished with five hundred weight emery paper prior to assembly.

The water which heats and cools the top and bottom disk assemblies respectively enters the rotating section through two Duoflow rotary unions. Early experiments were performed using electrical heating on top and water cooling on the bottom. However, a change was made to water heating for three reasons, viz. to minimize radial temperature gradients on the heated plate, to allow the apparatus to reach steady state more quickly, and to allow studies of heating from above and below to be made in the same apparatus. The heating (or cooling) water enters the heating water section, is forced radially outward between the aluminium surface and a horizontal plastic partition, then flows radially inward on the other side of the partition and finally out through the rotary union.

Temperatures were measured by means of thermistors which were installed prior to pouring the epoxy layers. These thermistors were embedded in grooves cut in the aluminium disks on the surfaces next to the epoxy layers, and were held with technical

|   | Low viscosity oil<br>(0.65 cS nominal)           | High viscosity oil<br>(350 cS nominal)         |
|---|--|--|
| †Density (g/cm <sup>3</sup> )   | 0.761  | 0.970  |
| †Coefficient of thermal expansion<br>(°C <sup>-1</sup> )                        | 0.00134  | 0.00096  |
| †Thermal conductivity [cal/(s cm °C)]   | 0.00024  | 0.00038  |
| †Specific heat, $C_p$ [cal/(g °C)]  | 0.349  | 0.349  |
| ‡Kinematic viscosity (cS) constants<br>for equation<br>$\log_{10} \nu = AT + B$ | $A = -0.002638 \text{ °C}^{-1}$<br>$B = -0.1211$ | $A = -0.006691 \text{ °C}^{-1}$<br>$B = 2.711$ |

† Value at room temperature supplied by manufacturer.  
‡ Determined by Ostwald viscometer technique.

TABLE 1. Physical properties of Dow Corning 200 fluid.

G cement having a high thermal conductivity. Six thermistors were embedded in the assembly as follows: no. 1 is immediately above the top epoxy layer, 2 and 3 are in the thin aluminium plate just above the test fluid, 4 and 5 are in the thin aluminium plate just below the test fluid, and 6 is in the lower thick aluminium plate. The leads for 2 and 3 are brought in in a groove adjacent to the epoxy layer and then through a hole in the top thin aluminium disk which approaches, but does not reach, the working fluid cavity. Numbers 4 and 5 are brought in in a similar way from below so that the silicone oil is in contact only with an unbroken aluminium disk. The thermistors are located one inch from the centre of the cylinder; numbers 1, 3, 5, and 6 are in a vertical line while 2 and 4 are displaced 15 degrees. The thermistor leads are brought out by means of a slip ring assembly. There are 10 solid coin silver slip rings and the brushes (three per ring) are silver graphalloy. Temperature drops across the epoxy layers and the working fluid as well as all individual temperatures were measured directly. The digital circuitry can measure directly the absolute temperature of a thermistor or the difference of any two thermistors with an accuracy of 0.015 °C. A seventh thermistor is used to measure the room temperature next to the rotating apparatus. The entire test cylinder was insulated with fibreglass wool.

Double bearings are used for both the top and bottom shafts in order to provide steady rotation. The two bearings on the bottom shaft (diameter = 0.813 inches) are radial thrust bearings while those on the upper shaft (diameter = 1.58 inches) are radial bearings. The apparatus was levelled using three adjustable bolts threaded into the bottom plate of a stationary frame. The radial and axial runouts of the bottom plate of the rotating assembly are less than 0.003 inch.

Properties of the Dow Corning fluids used in the study are given in table 1.

### 2.2. Procedure

The top and bottom surface temperatures were adjusted so that the mean of the two was approximately equal to the room temperature. Since the kinematic viscosity is evaluated at this mean temperature and the mean temperature did not vary greatly among experiments, runs at constant rotational rates are approximately equivalent to runs at constant Ekman number.

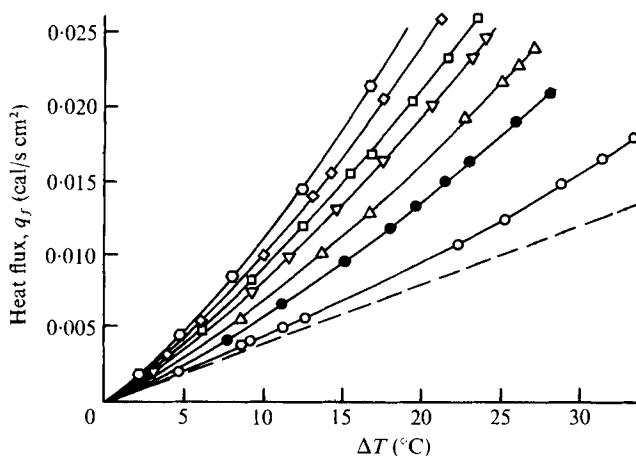


FIGURE 2. Heat flux as a function of temperature drop across the fluid, 350 cS oil,  $d = 0.97$  cm,  $\circ$ , 856 r.p.m.;  $\diamond$ , 691 r.p.m.;  $\square$ , 534 r.p.m.;  $\nabla$ , 440 r.p.m.;  $\triangle$ , 301 r.p.m.;  $\bullet$ , 210 r.p.m.;  $\circ$ , 102 r.p.m.; ---, 0 r.p.m.

The heat flux to the working fluid is obtained from measurements of temperature drops across the epoxy layers. The resistances of the epoxy layers were calibrated by making runs with a stationary cylinder filled with silicone oil and heated from above; under these conditions there is no convection. Conduction through both the stationary fluid and the plastic cylinder were included in the calculation, assuming that their conductivities are known. Since the final results are presented in normalized form, i.e. as a Nusselt number, or ratio of rate of heat transfer to rate of heat transfer without rotation, errors arising from using these conductivities are small. The heat flux with rotation is then obtained by using the mean of the temperature differences across the top and bottom epoxy layers.

In the above calibration it is assumed that the heat losses from the apparatus are independent of rotational rate. In order to test that assumption, runs were made at zero and 440 r.p.m. with the silicone oil replaced by a solid piece of Plexiglas. In this way heat transfer inside the apparatus would be independent of rotational rate while the heat-transfer coefficient governing heat losses to the surroundings would vary. The results of this study showed that the effect of rotation on measured heat flux errors due to heat losses is very small.

Details on the apparatus and procedure can be found in Tang (1975).

### 3. Results

#### 3.1. Viscous flow regime - 350 cS oil

Measurements were made at rotational rates of 0, 102, 125, 151, 175, 210, 251, 301, 440, 534, 691 and 856 r.p.m. for the cylinder of height 0.97 cm and 0, 102, 210, 300, 440, 534 and 692 r.p.m. for the cylinder of height 2.00 cm. Tables of experimental results are given in Tang (1975). Values are presented for measured quantities such as the temperature difference across the fluid ( $\Delta T_f$ ) and the mean temperature difference across the two epoxy layers ( $\Delta T_e$ ) and for calculated dimensionless groups such as Nusselt numbers ( $Nu$ ), thermal Rossby numbers ( $\beta$ ), and Ekman numbers ( $\epsilon$ ).

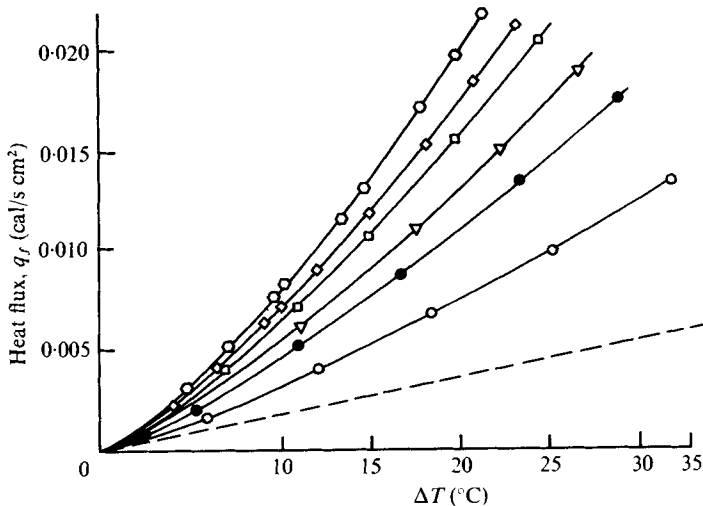


FIGURE 3. Heat flux as a function of temperature drop across the fluid, 350 cS oil,  $d = 2.0$  cm.  $\diamond$ , 692 r.p.m.;  $\diamond$ , 534 r.p.m.;  $\square$ , 440 r.p.m.;  $\nabla$ , 300 r.p.m.;  $\bullet$ , 210 r.p.m.;  $\circ$ , 102 r.p.m.; ---, 0 r.p.m.

The heat flux across the fluid as a function of the imposed temperature difference with the rotational rate as a parameter is shown in figures 2 and 3 for the two cylinders. Some rotational rates were omitted for ease of presentation. For the stationary cylinder the heat flux is a linear function of the imposed temperature drop, whereas with rotation the lines curve slightly upward.

As noted above, it can be shown that the Nusselt number should depend on five dimensionless parameters, viz. the Prandtl number  $\sigma$ , the Ekman number  $\epsilon$ , the thermal Rossby number  $\beta$ , the aspect ratio  $r_0$ , and the acceleration ratio  $Ac$  (Homsy & Hudson 1969). In the present study, the Prandtl number was not varied for either fluid. (The Prandtl number varies slightly, but not significantly, with small temperature changes. In addition, although the Prandtl numbers of the 350 cS and the 0.65 cS fluids are greatly different, the results for the two fluids must be treated separately owing to the differences in flow type. Therefore no information is obtained from these experiments on the dependence on  $\sigma$ .) Of the four remaining parameters, only three can be studied here, since, aside from slight variations in fluid properties, only the rotational rate, the imposed temperature difference across the fluid, and the cylinder height were varied in the experiments. According to theory, dependence on the acceleration ratio should be slight. Therefore we consider the dependence of the Nusselt number on the parameters  $\epsilon$ ,  $\beta$ , and  $r_0$ .

As noted in the introduction, the theory indicates that the Nusselt number may depend on a rotational Grashof number for non-boundary-layer flow, where the rotational Grashof number is defined by replacing the acceleration of gravity by the centrifugal acceleration at the outer edge of the cylinder. In terms of the dimensionless variables defined above

$$Gr_\omega = 32\beta r_0 / \epsilon^2. \quad (1)$$

The Nusselt number is shown as a function of  $Gr_\omega$  in figure 4. As can be seen, the fit is extremely good for all rotational rates and both cylinder heights, and a straight

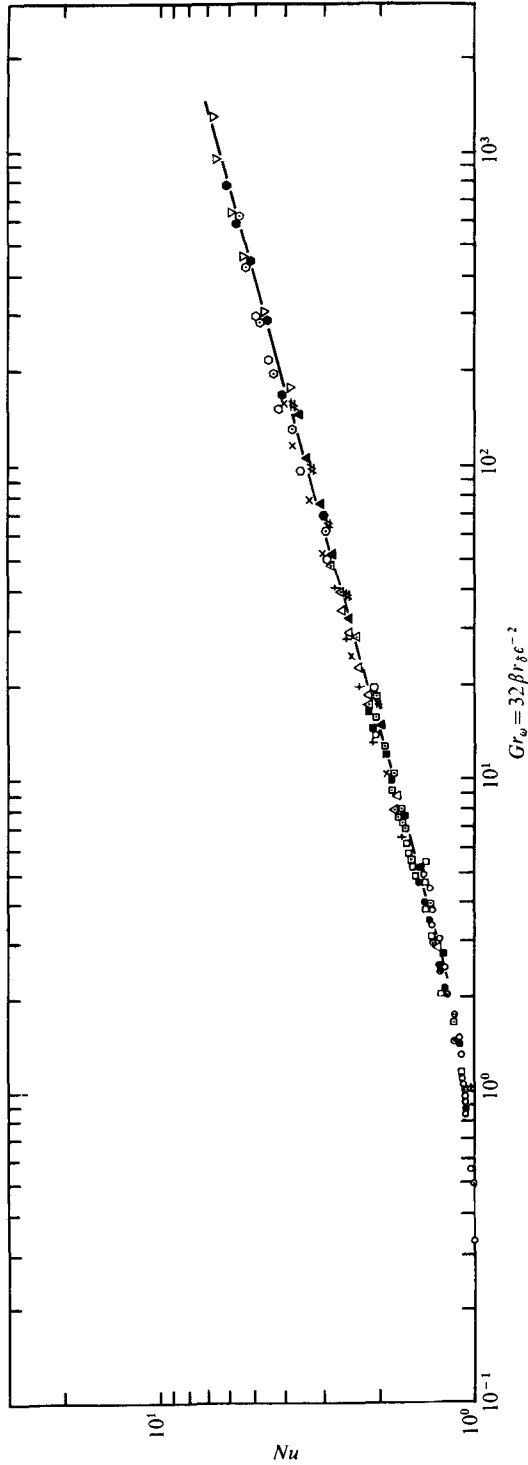


FIGURE 4. Nusselt number as a function of rotational Grashof number, 350 cS oil.  $d = 0.97$  cm:  $\circ$ , 102 r.p.m.;  $\odot$ , 125 r.p.m.;  $\bullet$ , 151 r.p.m.;  $\square$ , 175 r.p.m.;  $\square$ , 210 r.p.m.;  $\blacksquare$ , 301 r.p.m.;  $\triangle$ , 440 r.p.m.;  $\triangle$ , 534 r.p.m.;  $\blacktriangle$ , 691 r.p.m.;  $\ddagger$ , 856 r.p.m.  $d = 2.0$  cm:  $+$ , 102 r.p.m.;  $\times$ , 210 r.p.m.;  $\odot$ , 300 r.p.m.;  $\odot$ , 440 r.p.m.;  $\bullet$ , 534 r.p.m.;  $\nabla$ , 692 r.p.m.



line results for  $Gr_\omega \geq 2$ . The line shown in figure 4 was obtained from a regression analysis and is discussed further below.

A log-log plot such as figure 4 is, of course, rather insensitive to variations in the data. Therefore, in order to test further the dependence of the Nusselt number on the Ekman number, thermal Rossby number, and aspect ratio, a fit of the following form was sought:

$$Nu = \exp(E) \cdot \beta^A \cdot \epsilon^B \cdot r_0^D. \quad (2)$$

A multiple regression analysis was carried out for  $Gr_\omega \geq 2.0$  with the following results:

$$E = 1.19 \text{ (standard deviation} = 0.044),$$

$$A = 0.282 \text{ (standard deviation} = 0.0042),$$

$$B = 0.528 \text{ (standard deviation} = 0.0049),$$

$$D = 0.198 \text{ (standard deviation} = 0.014).$$

The standard error of estimate is 0.029 and the index of correlation is  $> 0.99$ . The results were based on 112 data points (108 degrees of freedom).

If the Nusselt number is to be a function only of the Grashof number, the exponents  $A$ ,  $B$ , and  $D$  must be related in a definite manner. By comparing (1) and (2),  $A$  and  $B$  should be related as  $B = -2A$  and  $D$  should be equal to  $A$ . To a very good approximation the desired relationship between  $A$  and  $B$  is satisfied. The exponent  $D$ , however, is somewhat less than the value of  $A$ . Therefore, the Nusselt number depends on the two groups  $(\beta\epsilon^{-2})$  and  $r_0$ ; this is equivalent to a dependence on  $Gr_\omega$  and  $r_0$ . As can be seen from (1) and (2), the Nusselt number can be considered to be a function of  $Gr_\omega$  and  $r_0$ . This possibility was examined by fitting an equation of the form

$$Nu = \exp(F) Gr_\omega^G r_0^H, \quad Gr_\omega \geq 2.0, \quad (3)$$

with the following values of the constants:

$$F = 0.126 \text{ (standard deviation} = 0.037),$$

$$G = 0.267 \text{ (standard deviation} = 0.0026),$$

$$H = -0.054 \text{ (standard deviation} = 0.012).$$

Equation (3) is based on 112 data points (109 degrees of freedom) and has an index of correlation  $\geq 0.99$  and a standard error of estimate of 0.031.

It can be seen from the result

$$Nu = 1.13 Gr_\omega^{0.267} r_0^{-0.054}, \quad Gr_\omega \geq 2.0, \quad (4)$$

that heat transfer for centrifugally driven thermal convection depends on the system parameters, particularly the imposed temperature difference and acceleration, much as in stationary natural convection. This occurs when boundary layers do not form, so that the Coriolis acceleration cannot dominate the interior flow.

An analysis of (4) was made to determine whether the exponent  $r_0$  ( $-0.054$ ) was statistically different from zero. An  $F$  test for removing a variable was carried out with the result  $F = 18$ . At  $\alpha = 0.05$ ,  $F(1, 109)$  is approximately 4. Thus the hypothesis,  $H = 0$  [in equation (3)], was rejected. Even though the assumption of normally distributed errors in the regression variables may not hold since the regression variables

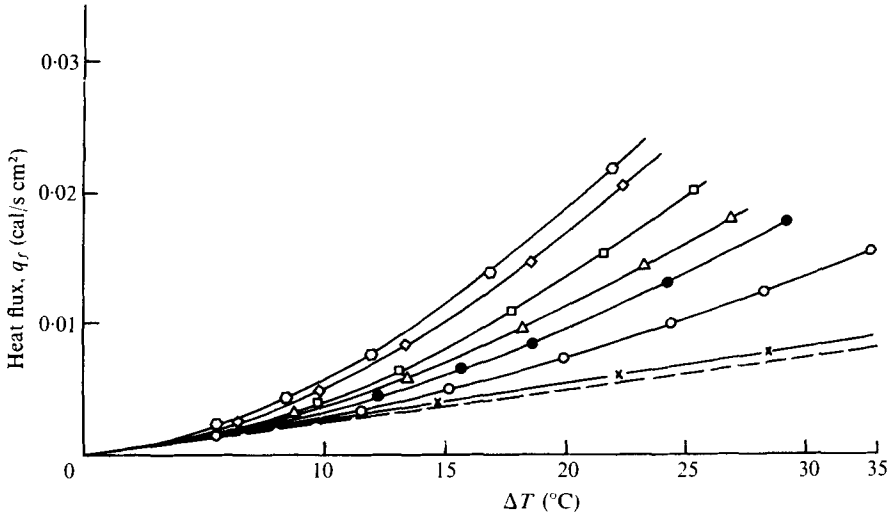


FIGURE 5. Heat flux as a function of temperature drop across fluid, 0.65 cS oil,  $d = 0.97$  cm.  $\diamond$ , 850 r.p.m.;  $\diamond$ , 696 r.p.m.;  $\square$ , 440 r.p.m.;  $\triangle$ , 300 r.p.m.;  $\bullet$ , 261 r.p.m.;  $\circ$ , 100 r.p.m.;  $\times$ , 27 r.p.m.; ---, 0 r.p.m.

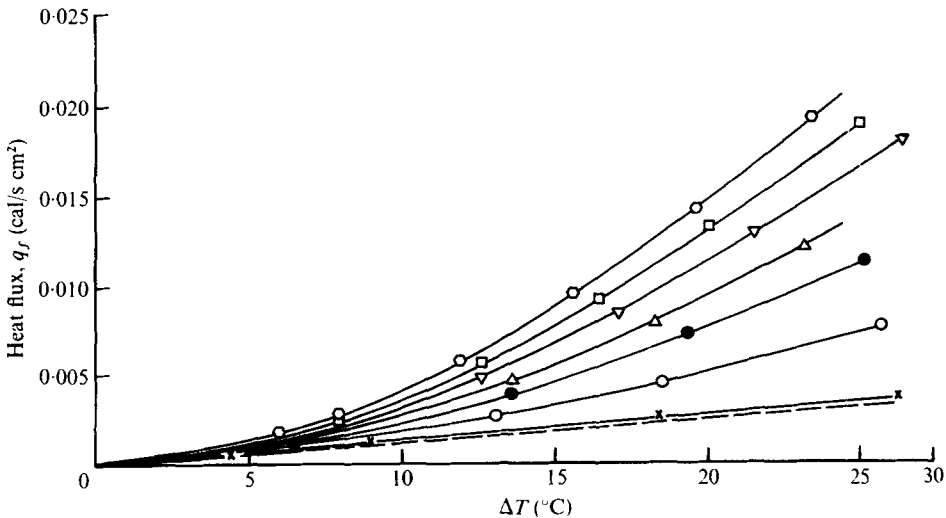


FIGURE 6. Heat flux as a function of temperature drop across fluid, 0.65 cS oil,  $d = 2.0$  cm.  $\circ$ , 690 r.p.m.;  $\square$ , 534 r.p.m.;  $\nabla$ , 440 r.p.m.;  $\triangle$ , 300 r.p.m.;  $\bullet$ , 200 r.p.m.;  $\circ$ , 100 r.p.m.;  $\times$ , 27 r.p.m.; ---, 0 r.p.m.

are logarithms of  $\beta$ ,  $\epsilon$ , and  $r_0$ , the difference between 18 and 4 is large enough such that the exponent  $-0.054$  may be considered significantly different from zero.

In general, then, the Nusselt number depends on the two parameters  $Gr_w$  and  $r_0$ . Thus two straight lines should be drawn on figure 4 for  $r_0 = 6.99$  and  $r_0 = 14.4$  ( $Gr_w \geq 2$ ). However, these two lines would be close together since  $r_0$  varies only by a factor of 2 in these experiments which causes the Nusselt number to vary by  $2^{0.054}$  or a factor of 1.04. Therefore, a single line is drawn in figure 4, eliminating the dependence on  $r_0$ .

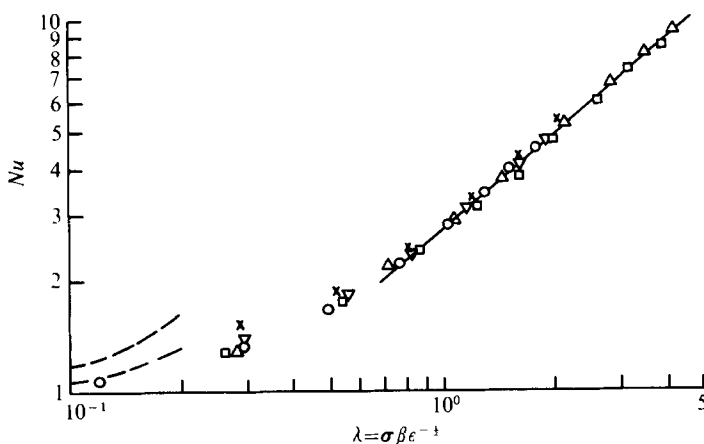


FIGURE 7. Nusselt number as a function of  $\lambda = \sigma\beta\epsilon^{-\frac{1}{2}}$ , 0.65 cS oil.  $d = 2.0$  cm:  $\triangle$ , 690 r.p.m.;  $\square$ , 534 r.p.m.  $d = 0.97$  cm:  $\times$ , 850 r.p.m.;  $\nabla$ , 696 r.p.m.;  $\circ$ , 527 r.p.m.; ---, equation (9).

This line was determined by performing a single-parameter regression analysis (rather than choosing a mean aspect ratio) resulting in

$$Nu = \exp(-0.0290) Gr_{\omega}^{0.274}, \quad Gr_{\omega} \geq 2.0, \quad (5)$$

where the standard deviations on  $-0.0290$  and  $0.274$  are  $0.0069$  and  $0.0019$  respectively, and the standard error of estimate is  $0.034$  and the index of correlation is  $> 0.99$ . The equation is based on 112 data points (110 degrees of freedom). Equation (5) is plotted in figure 4.

### 3.2. Ekman-layer regime - 0.65 cS oil

Measurements were made at rotational rates of 0, 19, 27, 44, 75, 100, 201, 300, 440, 527, 696, and 850 r.p.m. for height  $d = 0.97$  cm and 0, 27, 100, 200, 300, 440, 534, and 690 r.p.m. for  $d = 2.00$  cm. The heat flux as a function of temperature difference with selected rotational rates as parameters is shown in figure 5 ( $d = 0.97$  cm) and figure 6 ( $d = 2.00$  cm), and data are given in Tang (1975). The heat flux is enhanced over that obtained without rotation as the rotational rate is increased with the enhancement being small at 27 r.p.m.

As discussed in § 1, for sufficiently small values of  $\epsilon$ ,  $\beta$ , and  $Ac$  the Nusselt number should depend on the parameters  $\sigma$ ,  $\beta$ , and  $\epsilon$  as the group  $\sigma\beta\epsilon^{-\frac{1}{2}}$ ; furthermore, the dependence on the acceleration ratio  $Ac$  should be small (Homsy & Hudson 1969, 1971a). Thus the theory predicts that

$$Nu = Nu(\sigma\beta\epsilon^{-\frac{1}{2}}, r_0). \quad (6)$$

The theoretical results were obtained from perturbation analyses. It is of interest to determine whether equation (6) will hold under conditions obtainable in the laboratory.

The Nusselt number is shown as a function of  $\lambda \equiv \sigma\beta\epsilon^{-\frac{1}{2}}$  in figure 7 for values of the acceleration ratio  $Ac \leq 0.025$ ; Nusselt numbers for larger  $Ac$  do not fall on the curve. The straight line on the figure is given by

$$Nu = \exp(1.02) \lambda^{0.842}, \quad (7)$$

which was obtained from a regression analysis. The standard deviation in the exponent 1.02 is 0.0071 and in the exponent of  $\lambda$  is 0.011. The index of correlation is  $> 0.99$ . The analysis holds for  $\lambda \geq 0.70$  and is based on 27 data points (25 degrees of freedom). The standard error of estimate is 0.027.

The data seem to correlate well, but, as before, this is not a stringent test. We therefore carried out a multiple regression analysis of the data of the form of equation (2). Using figure 7 as a guide, we limited the correlation to  $Ac \leq 0.025$  and also to  $\lambda \geq 0.70$  since the curve appears linear for that range. The results of the regression analysis are, with  $A$ ,  $B$ ,  $D$ , and  $E$  defined by (2):

$$\begin{aligned} E &= 1.43 \text{ (standard deviation} = 0.35), \\ A &= 0.822 \text{ (standard deviation} = 0.0093), \\ B &= -0.499 \text{ (standard deviation} = 0.025), \\ D &= 0.173 \text{ (standard deviation} = 0.049). \end{aligned}$$

The standard error of estimate is 0.022 and the index of correlation is  $> 0.99$ . The analysis was based on 27 data points (23 degrees of freedom).

Thus for the 0.65 cS oil, the Nusselt number is given by

$$Nu = 4.16\beta^{0.822} \epsilon^{-0.499} r_0^{0.173}, \quad Ac \leq 0.025, \quad \lambda \geq 0.7. \quad (8)$$

It can be seen from a comparison of (8) and (6) that the theory predicts the relationship between the exponents of  $\beta$  and  $\epsilon$  rather well. The theory is based on a perturbation analysis for small  $\epsilon$  and  $\beta$  and the importance of higher-order terms is not completely determined. Although the exponent of  $\epsilon$  is not exactly minus one-half that of  $\beta$ , it is expected to approach that value as  $\epsilon$  and  $\beta$  approach zero.

The prediction given by (6) is thus substantiated by the experiments. It would also be of interest to determine whether the Nusselt numbers predicted by the theories are in agreement with experiment. The theory which is most closely related to the experiments described here is found in Homsy & Hudson (1971*a*), where the region  $\beta, \epsilon \leq 1$ ,  $Ac \ll (\lambda r_0)^{-1}$ ,  $r_0 \gg 1$ ,  $\lambda r_0 \leq O(1)$  was considered. The theory thus holds for large aspect ratios  $r_0$  but for small values of the parameter  $\lambda$ . Under these conditions the predicted Nusselt number for an insulated side wall is

$$Nu = 1 + 1.16r_0\lambda^2 - \frac{2}{3}\lambda^2. \quad (9)$$

Equation (9) was obtained from a perturbation analysis and is shown in figure 7 for the two values of  $r_0$  used in the experiments. The theory holds only for small  $\lambda$  and these are the conditions under which it is most difficult to obtain data since  $\lambda$  is proportional to  $\Delta T \omega^{\frac{1}{2}} d$  and at high rotational rates either  $\Delta T$  or  $d$  must be quite small. (The data point to the left of figure 7 was obtained with  $d = 0.97$  cm and at 527 r.p.m., i.e. the lowest values of both parameters used in the graph. The average temperature drop across the two epoxy layers was 0.22 °C.) Therefore, these experiments cannot be used to verify the prediction of (9). However, the experiments and theory do appear to be consistent. The experimental Nusselt numbers approach the correct value of one as  $\lambda$  approaches zero and probably agree with (9) for sufficiently small  $\lambda$ .

Finally, by comparing (8) and (3) the difference between a boundary-layer flow and a non-boundary-layer flow can be seen. In the former case the Nusselt number is a

function of  $\lambda = \sigma\beta\epsilon^{-\frac{1}{2}}$  and  $r_0$  whereas in the latter case it depends on  $Gr_\omega$  and  $r_0$  where  $Gr_\omega$  is the rotational Grashof number defined by (1).

#### 4. Conclusions

With the 350 cS oil, viscous forces are important throughout the cylinder and the Coriolis acceleration does not dominate the flow. Under these conditions the convection is analogous to stationary natural convection and the Nusselt number is a function of the rotational Grashof number as shown in (3).

For the 0.65 cS oil, boundary layers develop and the flow in the internal core region is controlled by the Coriolis acceleration. Convection is then produced by Ekman suction and the Nusselt number is given by (8), which is consistent with theories [equation (6)] obtained for the limit of  $\epsilon$  and  $\beta$  approaching zero.

Grateful acknowledgement is made to the National Science Foundation for partial support of this research through grants number NSF ENG 72-04081 to the University of Illinois and number NSF ENG 76-04345 to the University of Virginia. Acknowledgement is also given to Mr William Carpenter for his work on the statistical treatment of the data.

#### REFERENCES

- ABELL, S. & HUDSON, J. L. 1975 An experimental study of centrifugally driven free convection in a rectangular cavity. *Int. J. Heat Mass Transfer* **18**, 1415.
- BARCILON, V. & PEDLOSKY, J. 1967 On the steady motions produced by a stable stratification in a rapidly rotating fluid. *J. Fluid Mech.* **29**, 673.
- HOMSY, G. M. 1969 Centrifugally driven thermal convection and gravitational instabilities in bounded rotating fluids. Ph.D. dissertation, University of Illinois, Urbana-Champaign.
- HOMSY, G. M. & HUDSON, J. L. 1969 Centrifugally driven thermal convection in a rotating cylinder. *J. Fluid Mech.* **35**, 33.
- HOMSY, G. M. & HUDSON, J. L. 1971*a* Centrifugal convection and its effect on the asymptotic stability of a bounded rotating fluid heated from below. *J. Fluid Mech.* **48**, 605.
- HOMSY, G. M. & HUDSON, J. L. 1971*b* Heat transfer in a rotating cylinder of fluid heated from above. *Int. J. Heat Mass Transfer* **14**, 1149.
- LIGHTHILL, M. J. 1953 Theoretical considerations on free convection in tubes. *Quart. J. Mech. Appl. Math.* **6**, 398.
- LINDEN, P. F. 1977 The flow of a stratified fluid in a rotating annulus. *J. Fluid Mech.* **79**, 435.
- MATSUDA, T., HASHIMOTO, K. & TAKEDA, H. 1976 Thermally driven flow in a gas centrifuge with an insulated side wall. *J. Fluid Mech.* **73**, 389.
- NAKAYAMA, W. & USUI, S. 1974 Flow in rotating cylinder of a gas centrifuge. *J. Nuclear Sci. Tech.* **11**, 242.
- ROSSBY, H. T. 1969 A study of Bénard convection with and without rotation. *J. Fluid Mech.* **36**, 309.
- SAKURAI, T. & MATSUDA, T. 1974 Gasdynamics of a centrifugal machine. *J. Fluid Mech.* **62**, 727.
- SCHMIDT, E. H. 1951 Heat transmission by natural convection at high centrifugal acceleration in water-cooled gas-turbine blades. *General Discussion on Heat Transfer, Inst. Mech. Engrs, London*, pp. 361-363.
- TANG, D. K. 1975 Gravitational instabilities in a rotating fluid. Ph.D. dissertation, University of Illinois, Urbana-Champaign.
- TANG, D. K. & HUDSON, J. L. 1978 Gravitational instabilities in a rotating cylinder. In preparation.